

Rapidity distributions in high-energy nucleus-nucleus collisions

Shi Yafei,* Zhuang Pengfei, and Liu Lianshou

Institute of Particle Physics, Hua-Zhong Normal University, Wuhan, China

(Received 11 July 1989)

The rapidity distributions of shower particles in high-energy nucleus-nucleus collisions are investigated and compared with that in hadron-hadron and hadron-nucleus collisions. The remarkable difference in the correlation between rapidity distribution and multiplicity in the three cases, as well as the scaling of rapidity distribution in the target region and the nonscaling of the same distribution in the central region, are explained.

In recent years, a lot of data on the final states in high-energy nucleus-nucleus collisions have been obtained. In particular, the pseudorapidity distributions in the interaction of ^{16}O projectiles on AgBr, Au, W, etc., targets have been measured by the EMU-01, HELIOS, and WA80 Collaborations.¹⁻³ Some interesting results are the following.

(i) The correlation between rapidity distribution and multiplicity (or transverse energy) is weaker in nucleus-nucleus collisions as compared with that in hadron-hadron and hadron-nucleus collisions. As is well known,^{4,5} in $p\bar{p}$ collisions the peak of the rapidity distribution, being far from the midrapidity region for small multiplicity, smoothes down and shifts to the midrapidity region as the multiplicity increases, while in $p\text{-Pb}$ collisions the peak, being near the midrapidity region for small multiplicity, smoothes down and shifts towards the target-fragmentation region as the multiplicity increases. On the contrary, in ^{16}O -nucleus collisions^{1,2} the peak is essentially independent of multiplicity.

(ii) Similar to the limiting fragmentation in hadron-hadron collisions,⁶ there is evidence for the scaling property in the target-fragmentation region of nucleus-nucleus processes; i.e., the pseudorapidity distributions with the same target nuclei but different incident energies almost overlap in the $\eta < 1$ region.³

(iii) The rapidity distributions depend remarkably on the incident energy in the midrapidity region.³

The goal of this paper is to explain these experimental results, starting from the statistical model for particle production in high-energy collisions.⁷⁻¹² It is found that the hadron-hadron, hadron-nucleus, and nucleus-nucleus collisions can be described uniformly in the framework of the statistical model. The physical origin of the above-mentioned interesting features are readily understood.

The multisource model for high-energy hadron-nucleus and nucleus-nucleus collisions is a natural extension of the statistical model for hadron-hadron collisions. Its basic idea is the following. In high-energy hadron-nucleus and nucleus-nucleus processes, the interacting elements are the nucleons inside the nuclei. High-energy nucleus-nucleus collisions can be regarded as the folding of nucleon-nucleon collisions over the geometrical distribution of nucleons in nuclei.

According to this model, a nucleus-nucleus collision at

sufficiently high energy is a collision between the effective projectile (EP) and the effective target (ET), which are, respectively, the groups of the ν_{EP} nucleons in the projectile and the ν_{ET} nucleons in the target, participating in the collision. After the EP-ET collisions, one C^* , and several P^* and T^* systems are formed in different rapidity regions. We call these systems central fireball, projectile fireballs, and target fireballs, respectively. These systems ("fireballs") eventually hadronize into final-state hadrons. The number of nucleons in each EP and/or ET is determined by the geometry of the nuclei in collision. The numbers of P^* fireballs and T^* fireballs depend on the probability for the nucleons in the colliding nuclei to participate in nondiffractive collision. The multiplicity distributions of the fireballs depend on the numbers of energy sources for these fireballs.

In order to calculate the number of participants ν_{EP} and ν_{ET} , the Wood-Saxon distribution

$$p(r) = C \frac{4\pi r^2}{1 + \exp\left[\frac{r - r_0 A^{1/3}}{0.545}\right]} \quad (1)$$

for the nucleon distribution inside nucleus is used in this paper, instead of the uniform distribution used in Ref. 12. In Eq. (1), A is the mass number of the nucleus, r is the distance between the nucleon and the center of nucleus, r_0 is a parameter, and C is a normalization constant.

As is pointed out in Ref. 13, in the case of nucleus-nucleus collision, the probability for a nucleon to take place in a nondiffractive process is not the same as that for a nucleon-nucleon collision. Because of the nuclear geometry, a nucleon in the projectile (target) nucleus will encounter several target (projectile) nucleons. If the probability for a nucleon-nucleon collision to be diffractive is 0.25, after a number of collisions the probability will be highly reduced, and the corresponding nondiffractive probability will increase.¹³ The degree of this effect depends on the impact parameter b . In collisions with small b , each nucleon will go through a thick layer of nucleons and the nondiffractive probability is $W \approx 1$. On the contrary, in case of peripheral collisions, only a few nucleons are passed by the nucleon considered, and the nondiffractive probability will be $W \approx 0.75$. In general, $0.75 \leq W(b) \leq 1$. In the calculation of

$^{16}\text{O-Au,Ag}$ collisions we have taken

$$W(b) = \begin{cases} 1, & 0 \leq b < 2, \\ 0.8, & 2 < b \leq 5, \\ 0.75, & 5 < b \leq R_T + R_P - 1. \end{cases} \quad (2)$$

Thus the number of nucleons in the projectile and target nucleus taking part in nondiffractive collision is $\nu_P = W(b)\nu_{EP}$, $\nu_T = W(b)\nu_{ET}$, respectively. After the EP-ET collisions, one C^* fireball, $\nu_P P^*$, and $\nu_T T^*$ fireballs are formed.

The formation and decay of the C^* proceed as described in Ref. 12, i.e., its materialization energy is obtained randomly from $\mu_C = \nu_P + \nu_T$ energy sources. The corresponding multiplicity distribution for charged hadrons is

$$P_C(n_C | \mu_C) = \frac{1}{\Gamma(\mu_C)} \left[\frac{2}{\langle n_C^{hh} \rangle} \right]^{\mu_C} n_C^{\mu_C - 1} \times \exp \left[\frac{-2n_C}{\langle n_C^{hh} \rangle} \right], \quad (3)$$

where $\langle n_C^{hh} \rangle$ is the average charged multiplicity produced by the C^* fireball in nondiffractive hadron-hadron collision at the same incident energy.¹²

The formation and decay of P^* and T^* need some discussion. Since a nucleon in projectile or target may collide with many nucleons, the materialization energy of each P^* fireball is taken randomly from the energies of an incident nucleon and of the target nucleons hit by this nucleon. According to the straight-line geometry and the short-range property of nuclear forces, the number ν'_T of target nucleons colliding with an incident nucleon is just the number of nucleons inside a cylinder with an axis along the incident axis and a cross section approximately equal to πr_0^2 , where r_0 is the nucleon radius:

$$\nu'_T \simeq \frac{\nu_T}{S/\pi r_0^2}, \quad (4)$$

where S is the maximum overlapping cross section of the colliding nuclei at fixed b . Thus, the materialization energy of each P^* fireball is obtained randomly from

$$\mu_P = 1 + \nu'_T \beta \quad (5)$$

energy sources, where a parameter β is introduced to take into account the decreasing of interaction strength when the projectile nucleon pass through the target nucleus, $0 < \beta < 1$. The charged multiplicity distribution of each P^* fireball is

$$P_i(n_{P_i} | \mu_P) = \frac{1}{\Gamma(\mu_P)} \left[\frac{2}{\langle n_P^{hh} \rangle} \right]^{\mu_P} n_{P_i}^{\mu_P - 1} \exp \left[\frac{-2n_{P_i}}{\langle n_P^{hh} \rangle} \right], \quad i = 1, 2, \dots, \nu_P. \quad (6)$$

For the same reason, the materialization energy of each T^* fireball is obtained from the above formulas with the subscripts P and T exchanged.

As in the case of hadron-hadron collisions,⁹ we assume that, under the constraints of energy conservation and transverse-momentum cutoff, the rapidities of produced particles are distributed with equal probability. The inclusive rapidity distribution function in the rest frame of fireball satisfying this requirement is¹⁴

$$F_k(y) = K_k \left[\xi + \frac{\cosh y}{T_k} \right]^{-2}, \quad k = C, P_i, T_j, \quad (7)$$

where ξ is the transverse-momentum-cutoff factor, K_k is a normalization constant, and T_k is a characteristic parameter, "partition temperature," which depends only on the average multiplicity $\langle n_k^{hh} \rangle$ (Ref. 9).

The total rapidity distribution at fixed multiplicity n and impact parameter b is

$$\frac{dn}{dy}(b) = \int \left[n_C F_C(y - Y_C) + \sum_{i=1}^{\nu_P} n_{P_i} F_{P_i}(y - Y_{P_i}) + \sum_{j=1}^{\nu_T} n_{T_j} F_{T_j}(y - Y_{T_j}) \right] \times \frac{P_C(n_C | \mu_C) \prod_{i,j=1}^{\nu_P, \nu_T} P_i(n_{P_i} | \mu_P) P_j(n_{T_j} | \mu_T)}{P(n|b)} \delta \left[n - \sum_{i=1}^{\nu_P} n_{P_i} - \sum_{j=1}^{\nu_T} n_{T_j} \right] dn_C \prod_{i,j=1}^{\nu_P, \nu_T} dn_{P_i} dn_{T_j}, \quad (8)$$

where

$$P(n|b) = \int P_C(n_C | \mu_C) \prod_{i,j=1}^{\nu_P, \nu_T} P_i(n_{P_i} | \mu_P) P_j(n_{T_j} | \mu_T) \delta \left[n - \sum_{i=1}^{\nu_P} n_{P_i} - \sum_{j=1}^{\nu_T} n_{T_j} \right] dn_C \prod_{i,j=1}^{\nu_P, \nu_T} dn_{P_i} dn_{T_j}. \quad (9)$$

Averaging over all possible b values, we obtain the total rapidity distribution at fixed n :

$$\frac{dn}{dy} = C \int \frac{dn}{dy}(b) b db, \quad (10)$$

where $C = 1/\int b db$ is the geometrical normalization constant. Doing a further average over all possible n

values, we obtain the rapidity distribution eventually:

$$p(y) = \int \frac{dn}{dy} P(n) dn / \int P(n) dn, \quad (11)$$

where

$$P(n) = C \int P(n|b) b db \quad (12)$$

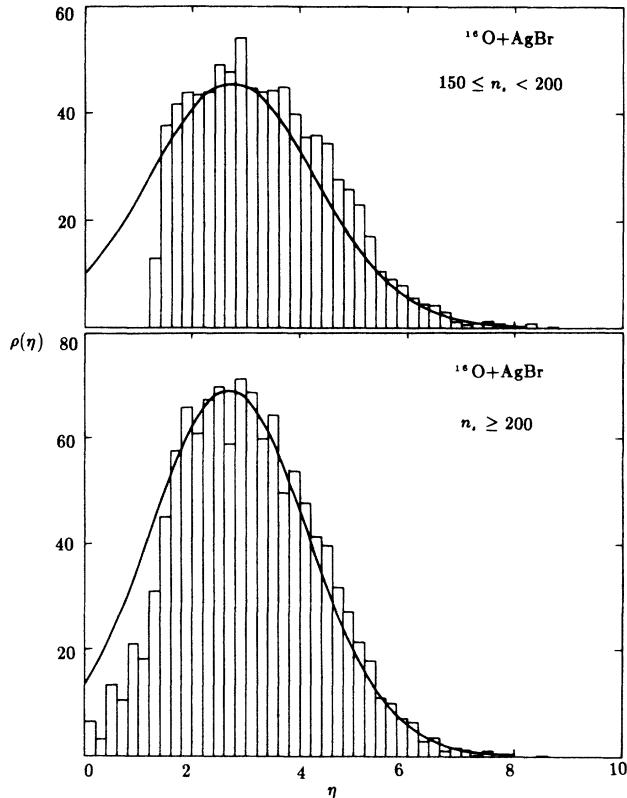


FIG. 1. The pseudorapidity distributions in $^{16}\text{O} + \text{AgBr}$ interaction at $200A$ GeV. The curves are the results of our model calculation. The data are taken from Ref. 1.

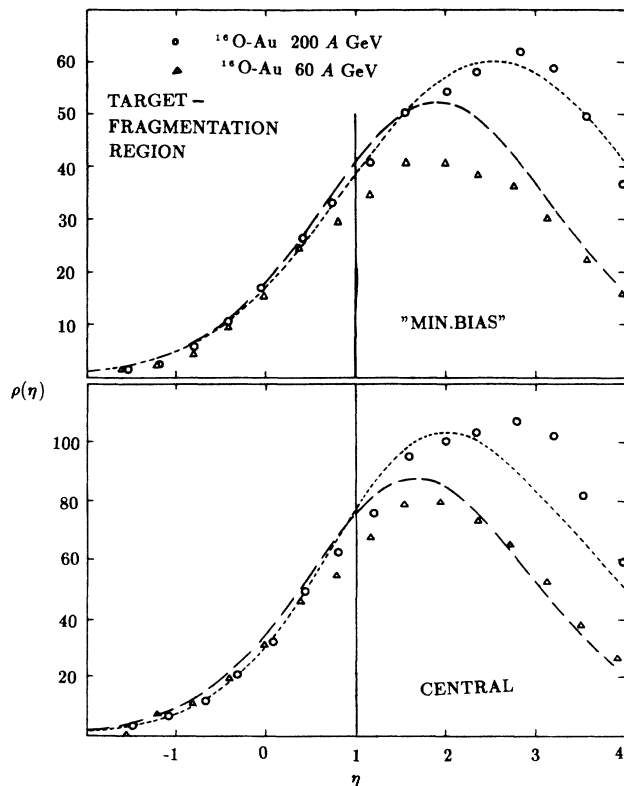


FIG. 2. The pseudorapidity distributions in $^{16}\text{O} + \text{Au}$ interaction for "minimum-bias" events and central events. The curves are the results of our model calculation. The data are taken from Ref. 3.

TABLE I. The partition temperatures for different incident energies.

	60 A GeV	200 A GeV
T_C (GeV)	0.25	0.64
$T_{P,T}$ (GeV)	0.5	0.53

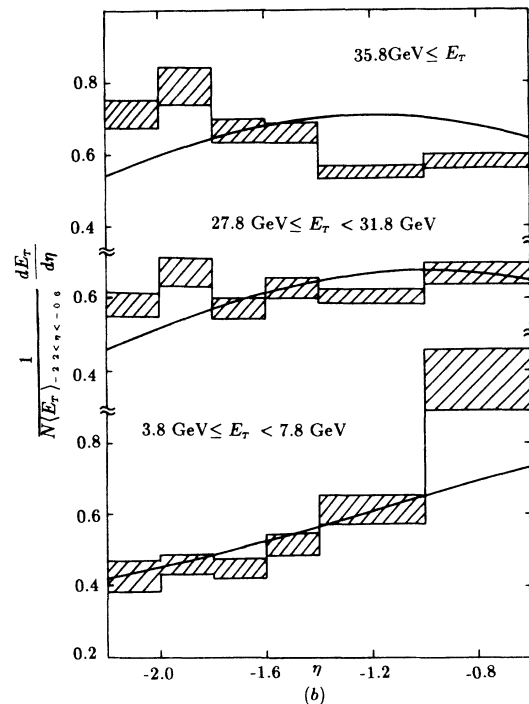
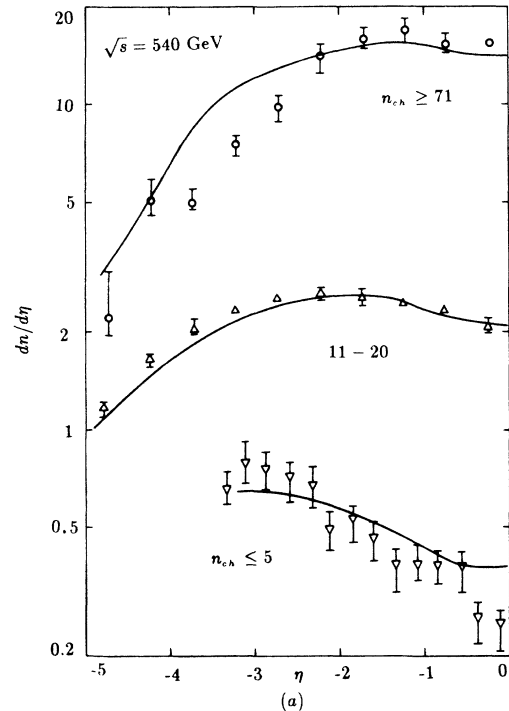


FIG. 3. (a) The pseudorapidity distributions in various multiplicities in $p\bar{p}$ collisions. The curves are the results of the three-fireball model calculation (in $p\bar{p}$ c.m.s.). The data are taken from Ref. 9. (b) The pseudorapidity distributions in various transverse energy E_T in $p\text{-Pb}$ collisions at 200 GeV/c incident hadron momentum. The curves are the results of the multisource model calculation (in pp c.m.s.). The data are taken from Ref. 11.

is the total multiplicity distribution of $\nu_P + \nu_T + 1$ fireballs.

In order to calculate the rapidity distribution, it is necessary to know the rapidities Y_k ($k=C, P_i, T_j$) of the fireballs. The charged multiplicities n_k and the rapidities Y_k of these fireballs satisfy energy-momentum conservation. In the EP-ET c.m. system (c.m.s.) we have

$$\begin{aligned} \frac{3}{2} \left[n_C \lambda_C \cosh Y'_C + \lambda_P \sum_{i=1}^{\nu_P} n_{P_i} \cosh Y'_{P_i} + \lambda_T \sum_{j=1}^{\nu_T} n_{T_j} \cosh Y'_{T_j} \right] \\ = (1-h)E, \\ n_C \lambda_C \sinh Y'_C + \lambda_P \sum_{i=1}^{\nu_P} n_{P_i} \sinh Y'_{P_i} + \lambda_T \sum_{j=1}^{\nu_T} n_{T_j} \sinh Y'_{T_j} \\ = 0, \end{aligned} \quad (13)$$

$$Y'_{T_j} < Y'_C < Y'_{P_i},$$

where h is the energy fraction taken away by the leading particles ($\approx \frac{1}{2}$); λ_k ($k=C, P, T$) is the average single-particle energy for partition temperature T_k ; and E is the total energy in the EP-ET c.m.s., which is related to the number of participants:

$$E = \nu_P m_N \cosh(y_L - y_C) + \nu_T m_N \cosh y_C, \quad (14)$$

where m_N is the mass of nucleon and y_L is the rapidity of incident nucleus in the laboratory reference frame. The EP-ET c.m.s. rapidity y_C is obtained by

$$\nu_{EP} m_N \sinh(y_L - y_C) + \nu_{ET} m_N \sinh(-y_C) = 0. \quad (15)$$

Obviously, the rapidities y_k of the $\nu_P + \nu_T + 1$ fireballs cannot be determined uniquely by Eqs. (13) alone. We make use of the following approximations.

(i) The rapidity of C^* is taken to be the same as EP-ET c.m.s. rapidity, so that $Y'_C = 0$ in the EP-ET c.m.s.; in the laboratory reference frame, $Y_C = y_C$, which is determined by Eq. (15).

(ii) Instead of the $\nu_P Y'_{P_i}$ and $\nu_T Y'_{T_j}$ we used their average values Y'_P and Y'_T , respectively. The Y'_P and Y'_T can be determined uniquely by Eq. (13). In the laboratory reference frame, $Y_P = y_C + Y'_P$, $Y_T = y_C + Y'_T$.

Using the model described above, we calculated the rapidity distributions in $^{16}\text{O-Au}$, AgBr , etc., collisions at 60 and 200 A GeV. The results are shown in Figs. 1 and 2. The values of partition temperature used in the calculation are listed in Table I.

It can be seen from Fig. 1 that the peaks of rapidity distributions with different multiplicities are located at essentially the same place. The position of the rapidity distribution peak does not move notably with the change of multiplicity as in the case of hadron-hadron and hadron-nucleus collisions. The physical origin of this phenomena is readily understood in our model. For hadron-hadron collisions, under the restriction of energy-momentum conservation, the small fireballs with low multiplicities fly rapidly, while the big fireballs with high multiplicities fly slowly. For this reason, the P^* fireball and the T^* fireball will shift towards the midrapidity region as the multiplicity rises, so that the peak in the rapidity distribution moves inward,⁹ Fig. 3(a). In hadron-nucleus collisions, there are ν_T T^* fireballs in the target-fragmentation region, but only one P^* fireball in the projectile-fragmentation region. The contribution of ν_T fireballs in the target-fragmentation region will be increasing notably as the multiplicity and/or transverse energy rises. It dominates not only over the contribution of the single P^* fireball, but also over that of the C^* fireball. It forces the peak of total rapidity distribution to shift toward the target-fragmentation region as the multiplicity rises,¹¹ cf. Fig. 3(b). In nucleus-nucleus collisions, however, there are ν_P P^* fireballs in the projectile-fragmentation region together with the ν_T^* fireballs in the target-fragmentation region. Their contributions compensate each other, so that the correlation between the position of the rapidity distribution peak and multiplicity is weakened.

It can be seen from Fig. 2 that the results of the multisource model reflect both the scaling property of the rapidity distribution in the target-fragmentation region and its energy dependence in the central region. The physical reason is clear. According to the model, high-energy nucleus-nucleus collisions can be regarded as nucleon-nucleon collisions plus nuclear geometry. The geometry is obviously independent of the incident energy, and it is known from the three-fireball model that the nucleon-nucleon collisions have a scaling property in the target-fragmentation region, while the contribution of the C^* fireball in the central region rises as the incident energy increases.¹⁵ For this reason, the rapidity distributions for the same projectile-target pair at different incident energies almost overlap in the target-fragmentation region, but differ remarkably in the central region.

This work was supported in part by the National Natural Science Fund of China.

*Permanent address: Yichang Teachers College, Yichang, China.

¹EMU-01 Collaboration, M. I. Adamovich *et al.*, Phys Lett. B **201**, 397 (1988).

²HELIOS Collaboration, T. Åkesson *et al.*, Z. Phys. C **38**, 383 (1988).

³WA80 Collaboration, I. Otterlund *et al.*, Report No. LUIP 8806, 1988 (unpublished).

⁴UA1 Collaboration, G. Arnison *et al.*, Phys. Lett. **123B**, 108 (1983).

⁵T. Åkesson *et al.*, Z. Phys. C **38**, 396 (1988).

⁶UA5 Collaboration, J. G. Rushbrooke *et al.*, in *Multiparticle Dynamics 1985*, proceedings of the XVIth International Symposium, Kiryat Anavim, Israel, 1985, edited by J. Grunhaus (World Scientific, Singapore, 1985).

⁷Liu Lianshou and Meng Tachung, Phys. Rev. D **27**, 2640 (1983).

⁸Chou Kuangchao, Liu Lianshou, and Meng Tachung, Phys. Rev. D **28**, 1080 (1983).

⁹Liu Liansou, Qin Lihong, and Zhuang Pengfei, Sci. Sin. A **29**,

- 1063 (1986).
- ¹⁰Cai Xu, Chao Weiqin, and Meng Tachung, *Phys. Rev. D* **36**, 2009 (1987).
- ¹¹Shi Yafei, Wang Zhengqing, and Zhuang Pengfei, *J. Central China Univ. Nat. Sci.* (to be published).
- ¹²Liu Lianshou, Meng Tachung, Pan Jicai, and Peng Hongan, *Phys. Rev. D* **38**, 3405 (1988).
- ¹³Miao Bixia and Chao Weiqin, Report No. BIHEP-TH-88-34, 1988 (unpublished).
- ¹⁴T. T. Chou, C. N. Yang, and E. Yen, *Phys. Rev. Lett.* **36**, 510 (1985).
- ¹⁵Wu Yuanfang and Liu Liansou, *Chin. Phys. Lett.* **3**, 517 (1986).